Available online at www.sciencedirect.com
SCIENCE DIRECT®
ELSEVIER
Journal of Molecular Catalysis A: Chemical 228 (2005) 145–150
JOURNAL OF MOLECULAR CATALYSIS A: CHEMICAL
www.elsevier.com/locate/molcata

Materials characterization by X-ray photoelectron spectroscopy

Pedro A.P. Nascente*

Universidade Federal de São Carlos, Departamento de Engenharia de Materiais, 13565-905 São Carlos, SP, Brazil

Available online 19 November 2004

Abstract

This paper deals with the application of the most used surface analysis technique on materials characterization, X-ray photoelectron spectroscopy (XPS). This spectroscopic technique employs low energy electrons as probes, since their mean free paths in the solids are only few atomic layers. Technologically interesting processes, in which the physical and chemical properties of the topmost atomic layers of the materials play an important role, include heterogeneous catalysis, thin film growth, surface segregation, corrosion, and tribology. Examples will be presented on the surface characterization of oxide catalysts, thin metallic films, and thin oxide films
© 2004 Elsevier B.V. All rights reserved.

Keywords: Surface analysis; Materials characterization; Photoelectron; XPS

1. Introduction

Nowadays, there are several surface analysis techniques that employ the interaction of photons, electrons, ions, or atoms with the material surface. In this paper, we concentrate on those techniques that utilize low energy electrons ($E < 1.5$ keV) as probing particles. These electrons are adequate to the investigation of surfaces because their inelastic mean free path in solids corresponds only to few atomic layers (0.5–3.0 nm) [1,2]. The most employed surface analysis techniques make use of these low energy electrons in one of the following manner: (1) impinging electrons cause the emission of backscattered and secondary electrons and (2) electrons are excited by impinging photons. The first case includes the emission of Auger electrons, while photoemission fits in the second case.

This paper is organized into four sections. In Section 2, a brief review of X-ray photoelectron spectroscopy (XPS) is presented. The instrumentation and experimental methodology are described in Section 3. The Section 4 comprises examples of materials characterization by XPS, including oxide catalysts, thin metallic films, ion nitrided iron, and thin oxide films. The summary is presented in Section 5.

2. X-ray photoelectron spectroscopy (XPS)

Photoelectron spectroscopy was developed by Siegbahn et al. at the University of Uppsala, Sweden, in the 1940s and 1950s, and was denominated electron spectroscopy for chemical analysis (ESCA) [3]. An electromagnetic source is used to eject electrons from the sample. Two conventional types of photon sources are used: a helium discharge lamp ($h\nu = 21.22$ and 40.8 eV for the HeI and HeII lines, respectively) and soft X-rays ($h\nu = 1253.6$ and 1486.6 eV for the Mg and Al Kα lines, respectively). Ultraviolet spectroscopy (UPS) makes use of the HeI and HeII lines, while XPS utilizes Mg and Al Kα lines. UPS is more adequate for investigating the valence band, and XPS has more widespread applications, being employed in the analysis of several types of materials, such as metals, polymers, ceramics, composites, semiconductors, and biological samples [1,2,4,5].

Since the energy levels are quantized, the photoelectrons have a kinetic energy distribution consisting of discrete peaks associated to the electron levels of the photoionized atom. The emitted electrons have a kinetic energy given by:

$$E_K = h\nu - E_B - \Phi \quad (1)$$

where E_K is the kinetic energy of the photoelectrons; $h\nu$, the incident photon energy; E_B, the electron binding energy; and Φ, the work function. Thus, E_B can be obtained by measuring

* Tel.: +55 16 2611229x217; fax: +55 16 2611160.
E-mail address: nascente@power.ufscar.br.

1381-1169/$ – see front matter © 2004 Elsevier B.V. All rights reserved.
doi:10.1016/j.molcata.2004.09.075

E_K. The identification of the elements present on the surface is done directly by the binding energies of the core photoelectrons. The intensity (integrated area under the photoelectron peak) is proportional to the atom quantity in the detected volume, allowing for a semiquantitative analysis of the surface [1,2,4,5].

The exact position of a photoelectron peak indicates the chemical state of the emitting atom, since the binding energies of the atom core levels are affected by its chemical environment. The change in binding energy is known as chemical shift, and it is due to the variations in the electrostatic screening sensed by the core electrons when the valence electrons of the emitting atom are attracted or repelled [1,2].

The photoelectron peaks appear in the spectrum superimposed on a background of secondary electrons. The presence of a core hole after the ionization affects the distribution of the emitted electrons, causing shifts, peak splitting, and the presence of satellites and shake-up lines [1,2,4]. The XP-spectrum also presents Auger electrons excited by X-ray [1,2]. Ghost peaks, which are caused by X-ray radiation from different material, can appear on the spectrum [2,4]. A commercial XPS apparatus usually employs a dual Al/Mg source, thus, it is possible to appear ghost peaks from Mg Kα radiation using the Al source, or the other way round [4].

3. Experimental

An XPS apparatus comprises an ultra-high vacuum chamber, an X-ray source, an ion beam gun, an electron gun, a sample manipulator, an electron analyzer, and a computer. An insertion device is used for changing samples without breaking vacuum. An ion beam gun is used for sample cleaning and for depth profiling analysis. The concentric hemispherical analyzer is the most used electron analyzer in XPS. It is necessary high resolution in electron energy (<0.1 eV) for those analyses in which the chemical shift must be measured accurately. Dielectric materials can be charged by the photoemission process, and their spectra shift up to 10 eV. A source of low energy electrons can be used to neutralize the sample charging.

The measurements reported in this paper were performed in ultra-high vacuum (low 10^{-9} Torr range) using a Kratos XSAM HS spectrometer. A dual Mg/Al anode was used as X-ray source. The high-resolution spectra were obtained with analyzer energy of 20 eV. The accuracy of the electron analyzer is 0.1 eV. Argon ion flux was employed to sputter the surface, if necessary. The Shirley background, Gaussian (for 1s peaks) and mixed Gaussian/Lorentzian (for p, d, and f peaks) functions, and a least-square routine were used for the fitting to the peaks. The binding energies were referenced to the hydrocarbon component C 1s level set at 284.8 eV. The sensitivity factors for quantitative analysis were referenced to $S_{F\,1s} = 1.0$, and their values are: 1.8 (Ti 2p), 10.0 (Ce 3d), 6.3 (Cu 2p), 4.5 (Ni 2p), 4.4 (Pt 4f), 7.2 (Sn 3d), and 0.66 (O 1s).

4. Applications in materials characterization

4.1. Oxide catalysts

XPS was used to investigate the chemical changes of the elements present at the surfaces of $CuO–TiO_2–CeO_2$ system synthesized by the sol–gel method [6,7]. The addition of CeO_2 on CuO supported by TiO_2 improves resistance to thermal loss of the supported catalyst surface area and helps to stabilize the active phase in a fine dispersed state [8]. A small addition of CeO_2 to the CuO/TiO_2 system increased the specific surface area of the catalyst, but as the amount of ceria increased, the surface area decreased, probably due to ceria segregation [7]. XPS analysis indicated that copper dispersion on the mixed support suffered no influence of cerium concentration, but it is dependent on the cerium species [6].

Fig. 1 displays the Ti 2p XP spectra of the catalysts and TiO_2-anatase (reference). The Ti 2p doublet of anatase and the $Ti_{0.91}O_{1.91}Cu_{0.09}$ sample presented its spin-orbit peaks, which could be well fitted by single component each, at 459.0 and 464.6 eV with relative areas (2:1), corresponding to Ti^{4+} in a tetragonal structure [6]. The spectra of samples containing CeO_2 were better fitted by two curves each peak, as can be seen in Fig. 2 for $Ce_{0.27}Ti_{0.64}O_{1.91}Cu_{0.09}$. The Ti $2p_{3/2}$ component at lower binding energy (459.3 eV) was assigned to titanium in a tetragonal structure, and the component at higher binding energy (460.5 eV), to a second Ti^{4+} species [6].

The Cu 2p spectra (not shown here) for the catalysts were very similar to that of CuO [7]. The Ce 3d spectra (not shown here) were deconvoluted by Ce^{4+} and Ce^{3+} components. The samples containing lower amount of ceria presented higher photoreduction due to the longer acquisition time required to improve the signal-to-noise ratio [6,7]. The CuO/TiO_2 system modified by CeO_2 presented a better performance for methanol dehydrogenation than the copper catalyst supported only on TiO_2 or CeO_2 [7].

4.2. Thin metallic films

Ultra-thin films of transition and noble metals present considerable interest in applications as catalysts and magnetic devices [9,10]. Films of copper, palladium, and gold were grown on polycrystalline substrates of the same metals (Cu/Pd, Cu/Au, Pd/Cu, Pd/Au, Au/Cu, and Au/Pd) [11]. The films were grown by DC sputtering, using a Balzers BA 510 instrument, with the following conditions: initial pressure of 4×10^{-5} Pa, partial pressure of argon of 0.4 Pa, sputtering current of 0.15 A, sputtering voltage of 0.9 kV, deposition rate of 0.05 nm/s, thickness of 10 nm, and deposition carried out at room temperature (approximately 300 K).

The morphology was investigated by atomic force microscopy (AFM), the structural characterization, by X-ray diffraction (XRD), and the surface analysis, by XPS. The AFM images of the Au and Pd substrate presented a smooth

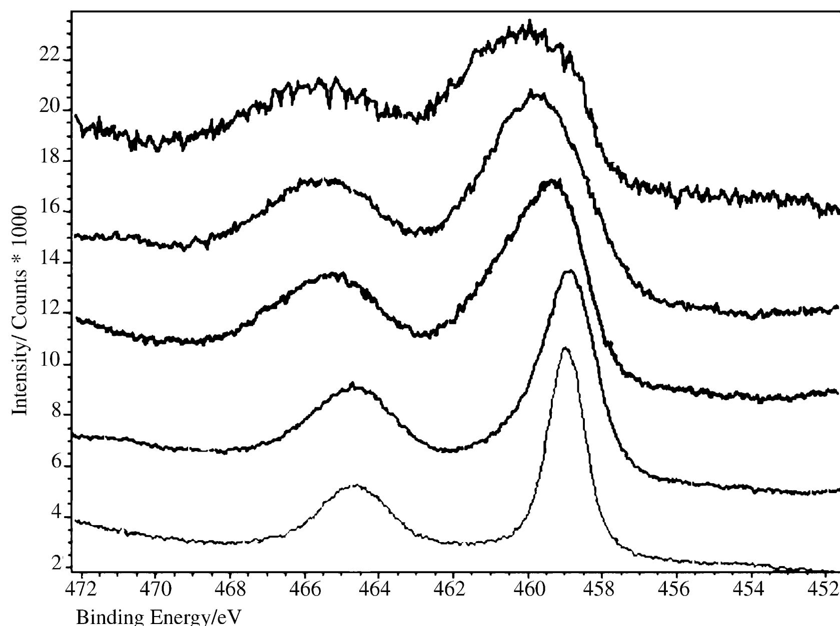

Fig. 1. Ti 2p XP spectra of (from bottom to top): TiO_2 (reference), $Ti_{0.91}O_{1.91}Cu_{0.09}$, $Ce_{0.09}Ti_{0.82}O_{1.91}Cu_{0.09}$, $Ce_{0.27}Ti_{0.64}O_{1.91}Cu_{0.09}$, and $Ce_{0.45}Ti_{0.46}O_{1.91}Cu_{0.09}$.

surface, with lines due to the rolling process. The morphology of the Cu substrate presented not only the lines but also small grains. The Au and Pd films on Cu presented similar morphologies, with a smoother aspect compared to the Cu substrate. The Pd/Au and Au/Pd films presented smooth morphologies, similar to the Au and Pd substrates. However, the Cu films on both Pd and Au presented surfaces covered by grains. The XRD results [12] indicated that the Cu/Pd and Cu/Au films were amorphous, while the Au films on both Cu and Pd were nanocrystalline. The Pd film presented a nanocrystalline structure on the Cu substrate, but an amorphous structure on the Au substrate.

The Cu 2p spectra are displayed in Fig. 3 for non-sputtered (a) and argon sputtered and (b) Cu films deposited on Pd [11]. For the sputtered film, the Cu $2p_{3/2}$ peak is located at 932.7 eV, corresponding to metallic Cu. For the non-sputtered film, there are two components for the Cu $2p_{3/2}$ peak, one at 932.6 eV and other at 934.5 eV. This component at higher binding energy can be attributed to CuO. The argon ion sputtering was effective in removing the oxide. Similar results

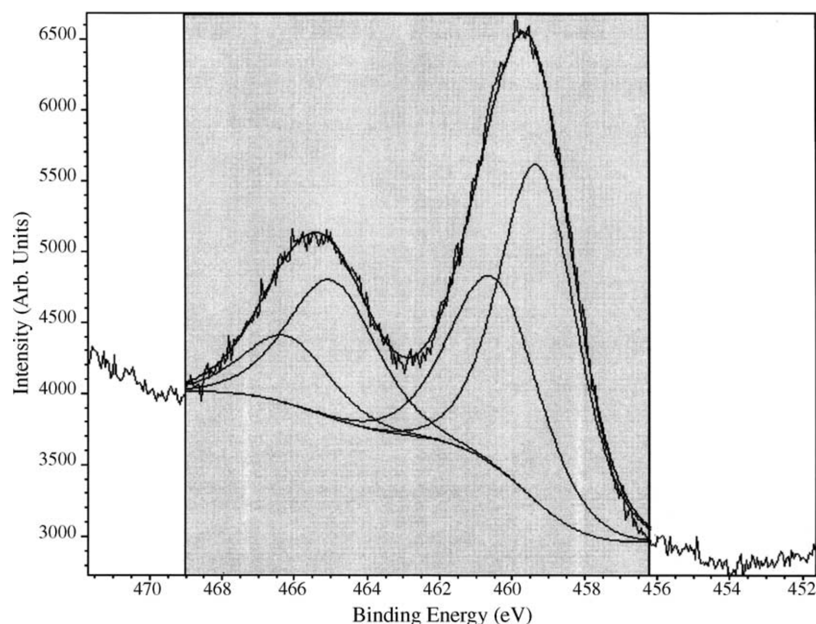

Fig. 2. Ti 2p XP spectrum of $Ce_{0.27}Ti_{0.64}O_{1.91}Cu_{0.09}$ showing the curve fitting.

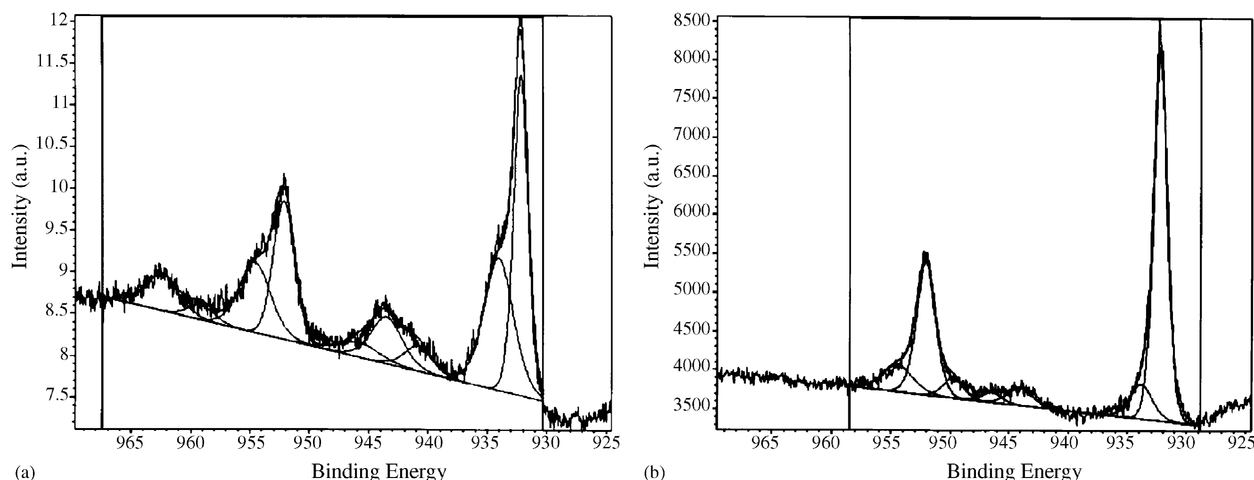

Fig. 3. Cu 2p spectra of Cu film on Pd (a) before and (b) after argon ion sputtering.

were obtained for the Cu film deposited on Au. For the other films, Pd/Cu, Pd/Au, Au/Cu, and Au/Pd, XPS did not detect oxidized surfaces; thus, suggesting that the grains observed by AFM were formed by copper oxide [11,12].

Films of nickel and palladium were grown on Pd and Ni substrates, respectively, by DC sputtering [13]. AFM, XRD, and XPS were employed in the characterization of the films. The AFM image of the Pd substrate displayed a smooth surface, with lines due to the rolling process, while the morphology of the Ni substrate presented grains in addition to the lines. The Ni film on Pd presented a surface covered by grains, and the Pd film on Ni presented a smoother surface than the Ni substrate. XRD results revealed an amorphous Ni film on Pd and a nanocrystalline Pd film on Ni [13].

Fig. 4 displays the XPS Ni 2p spectra of Ni/Pd (a) before and (b) after argon ion sputtering. In Fig. 3a, the Ni $2p_{3/2}$ component at approximately 852.5 eV correspond to metallic Ni, and the shoulder at higher binding energy can be deconvoluted by two peaks, at 854 and 856 eV, corresponding to NiO and Ni_2O_3, respectively. After the ion sputtering, the Ni spectrum corresponds to metallic nickel (Fig. 4b). For the Pd film deposited on Ni, the Pd 3d spectrum, not displayed here, obtained before and after argon ion sputtering corresponded to metallic palladium. There was no evidence of alloy formation for both cases, Ni/Pd and Pd/Ni [13].

The combined AFM, XRD, and XPS results for the metallic films deposited on transition metal substrates indicate that the morphological and structural properties of the films depend not only on the metal that is growing, but also on the morphology and composition of the substrate [11–13].

4.3. *Thin oxide films*

Pt modified SnO_2 electrodes were prepared in the form of thin films on titanium substrates by a sol–gel method, having a nominal composition of Sn/Pt = 1.5 (in atoms), at 200, 300, and 400 °C [14], and were characterized by SEM, XRD, and

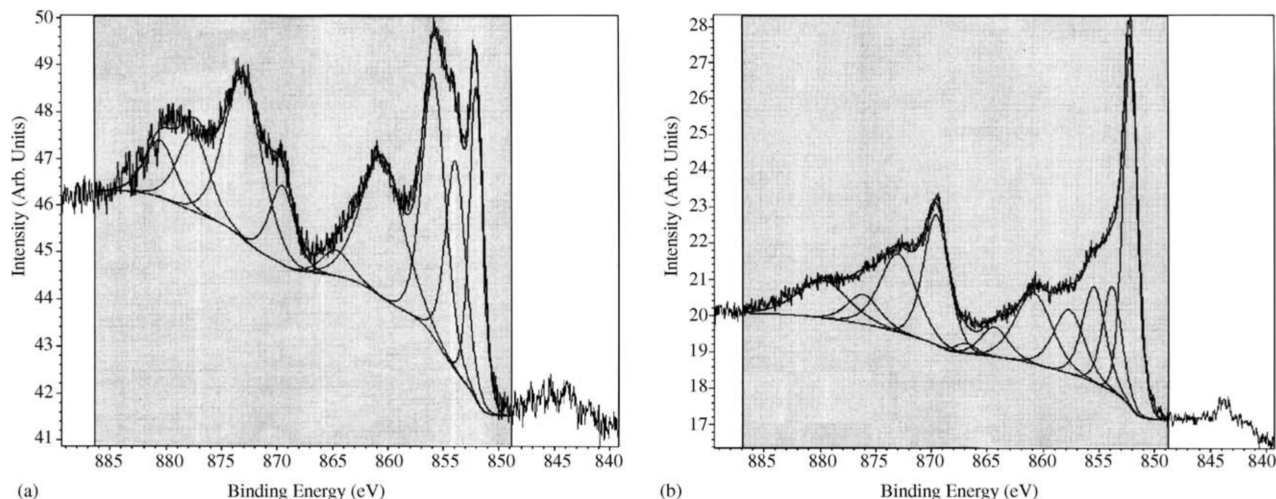

Fig. 4. Ni 2p spectra of Ni film on Pd (a) before and (b) after argon ion sputtering.

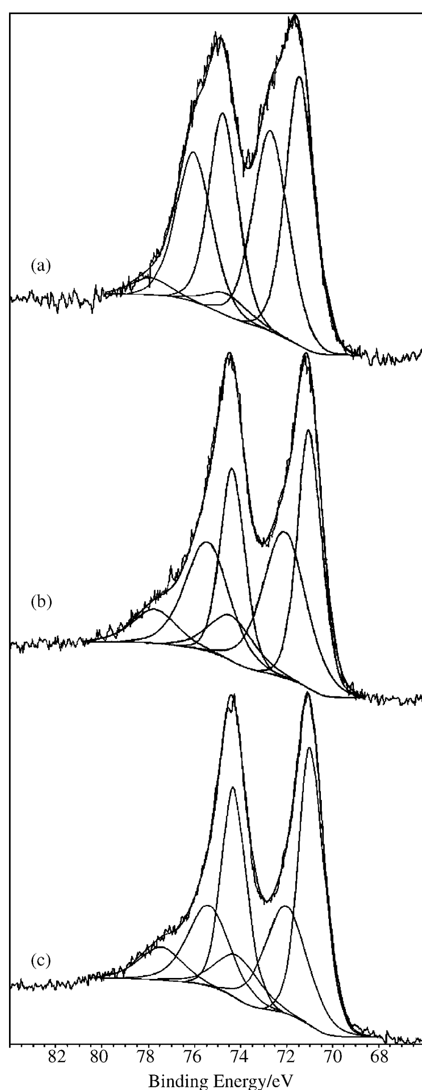

Fig. 5. Pt 4f spectra for Pt–SnO_2 films grown on Ti treated at the following temperatures: (a) 200, (b) 300, and (c) 400 °C.

XPS [14]. It was found that the Pt–SnO_2/Ti electrodes exhibit a significant catalytic activity for the oxidation of formaldehyde [14]. SEM and XRD results indicated that the films consisted of Pt nanoparticles dispersed into amorphous tin oxide.

Fig. 5 displays the Pt 4f spectra for Pt–SnO_2 films grown on Ti treated at the following temperatures: (a) 200, (b) 300, and (c) 400 °C. The Pt doublets could be deconvoluted into three components. The binding energies for the Pt $4f_{7/2}$ components are displayed in Table 1. The Sn 3d spectra of the three samples (not shown here) were similar and corresponded to oxidized tin. The XPS results suggested that Sn was present as SnO_2 and Pt was found in the zero-valence state (about 50%, Table 1) and in ionic form, probably as $Pt(OH)_2$ and PtO. The Sn/Pt ratio decreased from 1.6 for the film prepared at 200 °C to 0.5 and 0.6 for electrodes treated at 300 and 400 °C, respectively. So, the electrodes prepared at 200 °C presented a surface composition close to the nominal value (Sn/Pt ratio of 1.5), and those prepared at higher temperatures showed a significant Pt surface enrichment [17].

Table 1
Binding energies of the Pt $4f_{7/2}$ components for the Pt–SnO_2/Ti electrodes prepared at different temperatures

200 °C	300 °C	400 °C	Assignment
71.5 (49%)	71.0 (43%)	71.0 (52%)	Pt^0
72.7 (45%)	72.1 (43%)	72.1 (34%)	$Pt(OH)_2$
74.6 (6%)	74.4 (4%)	74.2 (14%)	PtO

The atomic percentages obtained from the relative contributions of each peak are in parenthesis.

5. Summary

This paper briefly describes the XPS technique and presents some applications on the characterization of oxide catalysts, thin metallic films, and thin oxide films.

Acknowledgements

I would like to thank my colleagues and students who contributed to the examples presented in Section 4. The work on CuO–TiO_2–CeO_2 catalysts was done in collaboration with Dr. Maria Suzana P. Francisco, Prof. Valmor R. Mastelaro, and Prof. Ariovaldo O. Florentino; on thin metallic films, with Ms. Larissa M.P. Pinheiro, Ms. Silvia S. Maluf, Dr. Angelo L. Gobbi, Prof. Pedro I. Paulin-Filho, and Prof. Márcia C.A. Fantini; on thin oxide films, with Prof. Hebe de las Mercedes Villullas, Dr. Flora I. Mattos-Costa, and Prof. Luiz O.S. Bulhões. Mr. Leon F. Feitosa helped with some of the figures. Financial support from the Brazilian agencies FAPESP, CNPq, and CAPES are gratefully acknowledged. This work was partially supported by the Brazilian Synchrotron Light Source (LNLS) under proposal MIC 2127.

References

[1] G. Ertl, J. Küppers, Low Energy Electrons and Surface Chemistry, VCH, Weinheim, 1985.
[2] D. Briggs, M.P. Seah (Eds.), Practical Surface Analysis, Wiley, Chichester, 1990.
[3] K. Siegbahn, et al., ESCA: Atomic, Molecular and Solid State Structure Studied by means of Electron Spectroscopy, Almquist & Wiksells, Uppsala, 1967.
[4] D.J. O'Connor, B.A. Sexton, R.St.C. Smart (Eds.), Surface Analysis Methods in Materiais Science, Springer-Verlag, Berlin, 1992.
[5] Y.-W. Chung, Practical Guide to Surface Science and Spectroscopy, Academic Press, San Diego, 2001.
[6] M.S.P. Francisco, P.A.P. Nascente, V.R. Mastelaro, A.O. Florentino, J. Vac. Sci. Technol. A 19 (2001) 1150.
[7] M.S.P. Francisco, V.R. Mastelaro, P.A.P. Nascente, A.O. Florentino, J. Phys. Chem. B 105 (2001) 10515.
[8] P.-O. Larsson, A. Andersson, J. Catal. 179 (1998) 72.
[9] C.T. Campbel, Ann. Rev. Phys. Chem. 41 (1990) 775.
[10] J.A. Rodriguez, Surf. Sci. Rep. 24 (1996) 223.

[11] S.S. Maluf, A.L. Gobbi, P.I. Paulin-Filho, P.A.P. Nascente, Surf. Interface Anal. 36 (2004) 931.

[12] S.S. Maluf, A.L. Gobbi, P.I. Paulin-Filho, P.A.P. Nascente, Thin Solid Films, submitted for publication.

[13] L.M.P. Pinheiro, S.S. Maluf, A.L. Gobbi, P.I. Paulin Filho, M.C.A. Fantini, P.A.P. Nascente, Thin Solid Films, submitted for publication.

[14] H.M. Villullas, F.I. Matos-Costa, P.A.P. Nascente, L.O.S. Bulhões, Electrochim. Acta 49 (2004) 3909.